

Experimental Evaluation of Fracture Models Parameters and its Validation for Naturally Aged Composite Solid Propellant

Deokumar Verma^{*,*}, Vivek Gaba[§], S. Bhowmick[§] and MVL Ramesh[#]

[#]DRDO-SF Complex, Jagdalpur - 494 001, India

[§]Department of Mechanical Engineering, National Institute of Technology, Raipur - 492 010, India

^{*}E-mail: deoverma.asl@gov.in

ABSTRACT

Parameters for the Fracture models namely the Inherent Flaw Model (IFM), Point Stress Criterion (PSC) and Average Stress Criterion (ASC) were experimentally determined for HTPB-Al-based composite Solid Propellant of three different compositions. A Compact Tension specimen with geometry, as suggested in ASTM-E399, was adopted to generate fracture data. Parameters were estimated from a zero-aged propellant and also from a propellant that was naturally aged up to 4 years. Failure Assessment Diagrams for composite propellants have been formulated based on Two Parameter Fracture Criterion (TPFC) for these three fracture models. The notched strengths estimated from the models agree with the experiment results. Measured fracture toughness values for aged propellant are less than un aged propellant. The estimated decrease in notch strength for three years naturally aged propellant (with an increase in crack size from 27 mm to 31 mm) for type-1, type-2 and type-3 propellant are 36.82 %, 39.90 % and 35.47 % respectively estimated from CT specimens. The study shows that the generated model can be utilized to predict the notched strength of cracked configuration in un-aged and aged HTPB-Al-based composite Solid Propellant.

Keywords: Solid propellant; Inherent Flaw Model (IFM); Point Stress Criterion (PSC); Average Stress Criterion (ASC); Failure Assessment Diagram (FAD)

NOMENCLATURE

K_I	: SIF in mode-I loading
K_{IC}	: Critical SIF in mode-I loading
c	: Initial crack length
ξ	: Ratio defined by c/w
P_Q	: Load corresponding to 95 % of the initial tangent
σ_N^∞	: Notch strength of the wide specimen
σ_N	: Notch strength of test CT specimen
K_Q	: Provisional fracture toughness as per ASTM E399
ρ_{ci}	: Characteristic length of IFM
σ_0	: Notch strength of the unnotched sample
ρ_{cp}	: Characteristic length of PSC
ρ_{ca}	: Characteristic length of ASC
K_Q^∞	: Fracture toughness of wide specimens in fracture models
K_f	: Parameter in fracture models
m	: Parameter in fracture models
SIF	: Stress intensity factor
LEFM	: Linear elastic fracture mechanics
IFM	: Inherent flaw model
PSC	: Point stress criterion
ASC	: Average stress criterion

1. INTRODUCTION

Solid propellant has proved its performance and reliability for its applications in Space and Defence over decades. With

the development of Defence technologies, the requirements for high-performance solid propellants with a high level of reliability over the entire duration of service life have been increased. One of the prime concerns is the initiation of micro flaws and cracks during storage and handling. The presence of micro flaws alters the mechanical behaviour and puts potential risks of its growth over time. If developed cracks exceed a certain limit, it restricts its usage as during the ignition/burning phase, these extra exposed surfaces (at the time of burning) will cause an unexpected rise in pressure resulting in catastrophic failure.

Review of propellant mechanical properties studied¹ for structural integrity. Since uniaxial testing is not adequate, numerous pioneer researchers have put their efforts into understanding and examining the fracture behaviour of solid propellants for years. Ha², *et al.* carried out studies for the strip-yield model and the Inherent Flaw Model conducting fracture toughness tests using CCT (Centre-Cracked Tension) specimens and Failure Assessment Diagram methods were investigated using these two models. Similar studies were carried out³ in polyamide12 resin. Shapery⁴, *et al.* established the theory of initiation and growth of cracks in viscoelastic media. Unique failure criterion for characterizing the fracture in solid propellant was studied and formulated⁵. The fracture process in solid propellant was examined experimentally through the J-integral concept⁶ and his co-workers. Effect of load history on fracture properties highlighted⁷. Further to this fracture behaviour was studied at various temperatures and strain rates⁸ and explained the dependency of fracture toughness

on these parameters. With the development of testing and computing efficiency, researchers developed fracture Criteria for solid propellant. Rao⁹⁻¹¹, *et al.* developed and experimentally validated fracture Criteria for solid propellant. Similar fracture models were developed and validated for laminate composite materials¹²⁻¹³. Attempts have been made to formulate fracture Criteria for composite and similar materials. Nuismer¹⁴, *et al.* formulated fracture Criteria for laminated composites containing stress concentration. Srivastava¹⁵, *et al.* studied load carrying capacity of laminate composite under different environment conditions. In the present study, parameters for fracture models were determined experimentally on solid propellant samples with three different compositions with ages ranging from un-age to naturally aged up to 4 years. Failure Assessment Diagrams were then evaluated from experimental data for these samples and results were compared. The rationale behind selection of the three fracture models namely IFM, PSC, and ASC is primarily to formulate fracture model which can predict fracture in solid propellants to a good level of accuracy and ease. Researchers too explored the adequacy of such models with specific compositions as evident in the Literatures.

The fracture models under study predicted the notched strength very closely within the domain of studies and close to the test results. Being polymeric material with apparently blunted zone close to crack tip, ASC can be an appropriate model for predicting fracture.

2. LEFMAND EXPERIMENTAL DETERMINATION OF FRACTURE TOUGHNESS FOR OPENING MODE

As per Linear Elastic Fracture Mechanics¹⁶, the stress field near the crack tip is fully characterized by Stress Intensity Factor in opening mode and is related to both stress and the size of the flaw.

The limiting value of SIF at onset crack propagation is a property of material known as fracture toughness. Fracture toughness K_{IC} (in opening mode) is a function of crack length and specimen geometry. As per procedures¹⁷ experimental determination of K_{IC} was carried out using Compact Tension (CT) specimens. Expression for provisional fracture toughness is expressed in Eqn. (1).

$$K_Q = \frac{P_Q}{B\sqrt{w}} f(\xi) \tag{1}$$

where: $\xi = \frac{c}{w}$; w being specimen width

$$f(\xi) = \frac{(2+\xi)}{(1-\xi)^{1.5}} (0.886 + 4.64\xi - 13.32\xi^2 + 14.72\xi^3 - 5.60\xi^4)$$

Once load P_Q is estimated from the experimented load line and displacement curve, provisional fracture toughness is estimated from Eqn. (1). The K_Q value estimated is valid K_{IC} if it meets the validity Criterion listed in Eqn. (2) through Eqn. (4). With ‘B’ being sample thickness.

$$B, c \geq 2.5 \left(\frac{K_Q}{\sigma_{ys}} \right)^2 \tag{2}$$

$$0.45 \leq \xi \leq 0.55 \tag{3}$$

$$P_{max} \leq 1.10P_Q \tag{4}$$

3. FORMULATION FOR FRACTURE STRENGTH AND CHARACTERISTIC LENGTH IN FRACTURE MODELS

With the development of polymer technology and its usage in propellant processing, efforts have been made over decades to understand and establish failure Criterion for Solid Propellant. Solid Propellant being a viscoelastic material undergoes changes in mechanical behaviour with time. From LEFM, SIF for infinite plate subjected to far-field stress is given by Eqn. (5).

$$K_I = \sigma \sqrt{\pi c} \tag{5}$$

There exists an intense energy region near the crack tip and applied successfully¹⁸ as it was applied to metal by Irwin. The resulting Eqn. is shown in Eqn. (6).

$$K_Q^\infty = \sigma_N^\infty \sqrt{\pi(c + \rho_{ci})} \tag{6}$$

In the Eqn. Above, σ_N^∞ is the fracture strength of a wide tensile specimen having a centre crack of length $2c$. This quantity $(c + \rho_{ci})$ is seen as an effective half-crack length. For the case of the unnotched specimen, the notched strength equals unnotched strength σ_0 and Eqn.(6) reduces to Eqn.(7).

$$K_Q^\infty = \sigma_0 \sqrt{\pi \rho_{ci}} \tag{7}$$

The quantity ρ_{ci} is then a half-crack length of an Inherent Flaw in the unnotched tensile specimen. Accordingly, the model in the literature is referred to as the Inherent Flaw Model (IFM). A schematic of stress intensified zone for IFM is shown in Fig. 1(a).

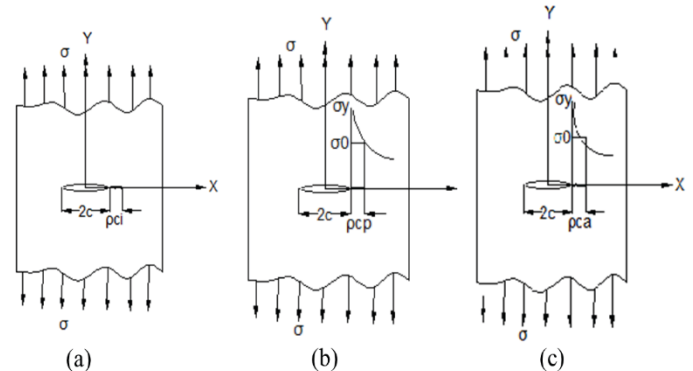


Figure 1. Schematic stress intensified zone for (a) IFM; (b) PSC; and (c)ASC.

The fracture strength (σ_N^∞) of the wide tensile specimen is obtained experimentally from test CT samples with a size correction factor of $f(\xi)$ ie ($\sigma_N^\infty = \sigma_N f(\xi)$). Further, combining Eqn. (6) & Eqn. (7), results in:

$$\frac{c + \rho_{ci}}{\rho_{ci}} = \left(\frac{\sigma_0}{\sigma_N^\infty} \right)^2 \tag{8}$$

From Eqn. (6), notched strength can be written as

$$\sigma_N^\infty = \frac{K_Q^\infty}{\sqrt{\pi(c + \rho_{ci})}} \tag{9}$$

An expression for the length of the intense energy zone ρ_{ci} (characteristic length) is written from Eqn. (8) as

$$\rho_{ci} = \frac{c}{\left(\frac{\sigma_0}{\sigma_N^\infty} \right)^2 - 1} \tag{10}$$

The fracture model, Point Stress Criterion (PSC) is based on the assumption that failure occurs when the applied normal stress $\sigma_y > 0$ over an axial distance of ρ_{cp} away from the crack

tip equals unnotched strength σ_0 . The schematic view of the failure Criterion is shown in Fig. 1(b).

$$\sigma_y(x, 0) \Big|_{x=c+\rho_{cp}} = \sigma_0 \tag{11}$$

Similarly, the fracture model Average Stress Criterion (ASC), is based on the assumption that the failure occurs when the average stress over an axial distance of ρ_{ca} ahead of the crack tip equals σ_0 . The schematic view of the failure Criterion is shown in Fig. 1(c).

$$\frac{1}{\rho_{ca}} \int_c^{c+\rho_{ca}} \sigma_y(x, 0) dx = \sigma_0 \tag{12}$$

The normal stress $\sigma_y > 0$ along the x-axis ahead of the crack is given by Eqn. (13).

$$\sigma_y(x, 0) = \frac{K_I x}{\sqrt{\pi c(x^2 - c^2)}}, x > c \tag{13}$$

Application of Eqn. (13) to fracture Criteria result in fracture strength relations

$$\frac{\sigma_N^\infty}{\sigma_0} = \sqrt{1 - \left(\frac{c}{c+\rho_{cp}}\right)^2} \tag{14}$$

For the Point Stress Criterion, and

$$\frac{\sigma_N^\infty}{\sigma_0} = \sqrt{\frac{\rho_{ca}}{2c+\rho_{ca}}} \tag{15}$$

For the Average Stress Criterion.

In the literature¹¹, it is noticed that the characteristic lengths in the fracture models are dependent on the notch sizes and are not the material constants. While it is argued¹⁹ that these are essentially constant values. In the present study, within the crack length studied, the characteristic lengths are experimentally determined and are apparently constant values. Two parameter fracture Criterion as suggested¹⁰⁻¹² are considered here for study. A linear relation between the two fracture parameters namely K_f and m is written as

$$K_Q^\infty = K_f \left\{ 1 - m \left(\frac{\sigma_N^\infty}{\sigma_0} \right) \right\} \tag{16}$$

The terms K_f and m in Eqn. (16) are determined by the least square fit to the data of K_Q^∞ , σ_N^∞ and σ_0 . The value of $m=0$ implies that K_f is equivalent to Linear Elastic Stress Intensity Factor K_1 and the Eqn. Applies to low toughness material. If the value of m is set to unity, the result applies to high-toughness material. If the value of m is found to be negative it is set to zero and the value of K_f is determined. Hence in the present analysis value of m is set between zero and unity. The value of K_f is determined by the least square for $0 \leq m \leq 1$. For the determination of K_f and m , a minimum of two notched samples and one unnotched sample are to be tested as recommended in the literature. Normally more samples are tested to cater for the dispersion in test results between samples. In the present studies, a minimum of three identical samples were tested at each test condition meeting the requirements¹⁷ of extracted from the same batch of materials.

As, $K_Q^\infty = \sigma_0 \sqrt{\pi \beta}$ where β is the characteristic length of the fracture models. The Eqn. (16) is arranged and re-written in non-dimensional form as

$$\sqrt{\frac{\beta}{\beta^*}} + m \left(\frac{\sigma_N^\infty}{\sigma_0} \right) = 1 \tag{17}$$

where

$$\beta^* = \frac{1}{\pi} \left(\frac{K_f}{\sigma_0} \right)^2$$

Or

$$m^2 \left(\frac{\sigma_N^\infty}{\sigma_0} \right)^2 - 2m \left(\frac{\sigma_N^\infty}{\sigma_0} \right) + \left(1 - \frac{\beta}{\beta^*} \right) = 0 \tag{18}$$

Once β^* and m in Eqn. (17) or Eqn. (18) are known, notched strength is easily determined for specific crack length by solving these non-linear equations by numerical methods like the Newton-Raphson method.

$$K_Q^\infty = K_f \left\{ 1 - m \left(\frac{\sigma_N^\infty}{\sigma_0} \right) \right\} X \sqrt{1 - \left(\frac{\sigma_N^\infty}{\sigma_0} \right)^2} \tag{19}$$

$$K_Q^\infty = K_f \left\{ 1 - m \left(\frac{\sigma_N^\infty}{\sigma_0} \right) \right\} X \sqrt{1 - \left(\frac{\sigma_N^\infty}{\sigma_0} \right)^2 + \sqrt{1 - \left(\frac{\sigma_N^\infty}{\sigma_0} \right)^2}} \tag{20}$$

$$K_Q^\infty = \frac{1}{\sqrt{2}} K_f \left\{ -m \left(\frac{\sigma_N^\infty}{\sigma_0} \right) \right\} X \sqrt{1 - \left(\frac{\sigma_N^\infty}{\sigma_0} \right)^2} \tag{21}$$

Relations for Failure Assessment Diagrams (FAD) for three fracture models are obtained by eliminating characteristic length in Eqn. (17) or Eqn. (18) with relations in Eqn. (8), Eqn. (14), Eqn. (15). The obtained relations for FAD of three models ie IFM, PSC and ASC are listed in Eqn. (19), Eqn. (20), Eqn. (21) respectively. The relations are significant as these can be utilized further for notched strength prediction in the tension of cracked configurations other than the centre crack²⁰. Establishing such fracture models has the advantage that these models can be used for the estimation of notch strength prediction of configurations other than standard specimen geometries.

4. SAMPLE SELECTION AND PREPARATIONS

All experiments were carried out on Compact Tension (CT) specimens as per ASTM E399 from HTPB-AP-Al based composite propellant with poly urethane-based curator with NCO to OH ratio of 0.80-0.85. The number average molecular weight of HTPB in selected propellant has values between 3000-5000. Hydroxyl values are in the range of 40-50 mg KOH/g. Ammonium Perchlorate in bi-modal form has particle size varying from 45-500 microns and 30-100 microns for type-1, it is 45-300 microns and 30-100 microns for type-2. Type-3 has a trimodal AP composition with a third particle size range (as compared to type-1) is 6-10 microns. Al powder has a

Table 1. Sample selection

Conditions	Type-1	Type-2	Type-3
HTPB	10	10	10
Al	18	18	19
AP	68	68	67
Catalyst	0.2	0.0	0.5
Others	3.8	3.5	3.5

size in the range of 16-20 microns. The compositions for three different propellant samples are listed in Table 1. Propellants are cast under vacuum and cured at 50 °C. CT specimen prepared as per¹⁷ for fracture testing.

The dimensions adopted for the present study for the specimen are shown in Fig. 2(a). The sample from the propellant finally prepared is shown in Fig. 2(b). After final punching pre-crack of known length was introduced in the samples by a new sharp razor blade.

Similar procedures have been adopted in literature⁵⁻²¹. The generated crack was observed in the high-resolution microscope with 200x and the pic from one of the samples is shown in Fig. 3. For each type of propellant under study, samples selected with naturally aged at ambient conditions ranging from un-aged, aged for 2 years, 3 years and 4 years. CT samples were tested in a Universal Testing Machine at cross-head speeds of 0.5 mm/min, 5 mm/min, 50 mm/min, 250 mm/min and 500 mm/min with an ξ value of 0.537.

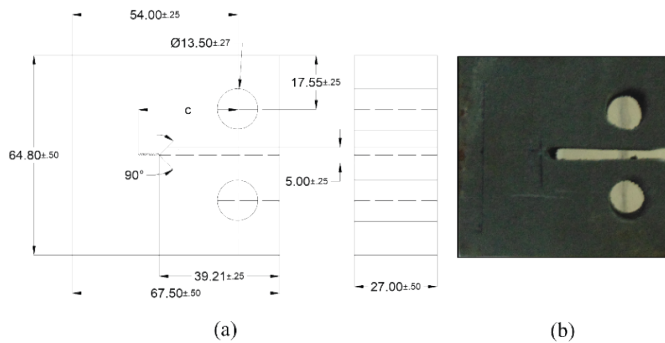


Figure 2. CT specimen as per ASTM E399 (a) Geometry with dimensional details; (b) Propellant CT Specimen.

A minimum of three samples were tested at each test condition. Provisional fracture toughness was evaluated for each sample and taken average. Tests were also carried out on three years aged samples with ξ from 0.482 to 0.574 at a cross-head speed of 50mm/min. Load and load line displacement for all test conditions recorded electronically.

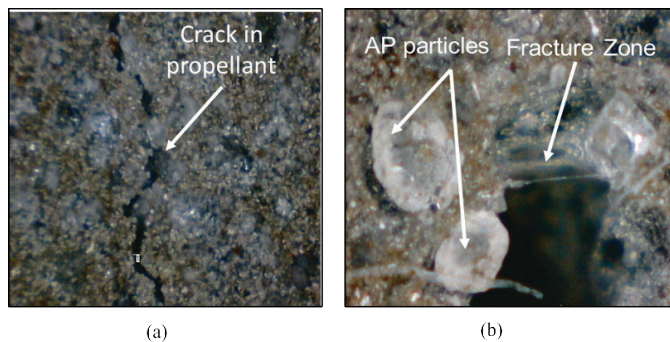


Figure 3. Crack growth in propellant (a) magnified view 200x; and (b) Fracture Zone during crack propagation.

During testing images of the fracture zone and crack front were recorded and shown in Fig. 3(a) and Fig. 3(b) respectively for one of the samples. The pictures clearly show the propagation of crack in heterogenous solid propellant in slight zig-zag manner. Propagation of crack is resisted by the strength of the binder while oxidizer particles get separated out during the phenomena. The more the binder filler strength, the more resistance it offers for crack growth.

5. RESULTS AND DISCUSSION

5.1 Effect of strain rate and ageing on fracture toughness of solid propellant

K_{IC} was evaluated from experiments at different strain rates for type-3 solid propellant samples under studies plotted against log strain rate in Fig. 4(a) with fitted curve.

$$K_{IC} = A1(\ln\dot{\epsilon})^2 + A2(\ln\dot{\epsilon}) + A3 \tag{22}$$

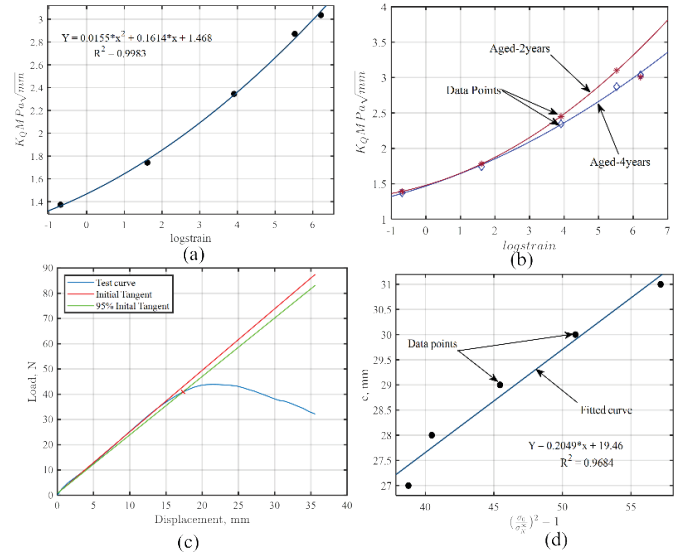


Figure 4. Propellant fracture toughness variation of K_{IC} with strain rates; (b) Variation of K_{IC} with age; (c) Load displacement curve; and (d) Characteristic length for IFM type-3 unaged.

In the graph, experiment data excellently fits with second order polynomial as in Eqn.(22) with r-square value of 0.998.

The same trends were noticed for samples of all test conditions. Test results for all three types two years of age and four years of age are shown in Table 2 and Table 3 respectively.

Table 2. Fracture toughness values evaluated with various crosshead speeds for naturally aged 2 years samples from CT specimen with c=29 mm, W=54 mm and B=27 mm.

Crosshead speeds (mm/min)	K_{IC} MPa√mm		
	Type-1	Type-2	Type-3
0.5	1.3924	1.0405	1.4025
5	1.7830	1.5214	1.7098
50	2.4520	1.8627	2.1554
250	3.0993	2.5383	2.7827
500	3.0066	2.5679	2.8545

From the curve fitting, the constant in Eqn. (22), evaluated and compiled in Table 4 and Table 5.

With age, the fracture toughness of solid propellant under study shows decreasing. The decrease is reflected in all tested strain rates. Evaluated fracture toughness is compared for 2-year and 4-year naturally aged samples for type-1 propellant in Fig. 4(b).

Failure load and the equivalent failure stress for the wide specimen for Type-1 propellant compiled and shown in Table 6.

Table 3. Fracture toughness values evaluated with various crosshead speeds for naturally aged 4 years samples from CT specimen with c=29 mm, W=54 mm and B=27 mm.

Crosshead speeds (mm/min)	K_{Ic} MPa \sqrt{mm}		
	Type-1	Type-2	Type-3
0.5	1.3732	1.3909	1.3074
5	1.7426	1.6448	1.6206
50	2.3453	1.9267	2.1247
250	2.8711	2.9617	2.7847
500	3.0360	2.6323	3.0581

Table 4. Experimentally evaluated values for constants in Eqn. 22 for naturally aged 2-year samples.

Conditions	A1	A2	A3	r ²
Type-1	0.0003	0.2229	1.5140	0.9856
Type-2	0.0106	0.1554	1.1680	0.9898
Type-3	0.0194	0.1122	1.4700	0.9898

Table 5. Experimentally evaluated values for constants in Eqn. 22 for naturally aged 4-year samples.

Conditions	A1	A2	A3	r ²
Type-1	0.0155	0.1614	1.4680	0.9983
Type-2	0.0213	0.0564	1.4400	0.9909
Type-3	0.0295	0.0899	1.3660	0.9983

Table 6. Experimentally evaluated failure load and failure stress for type-1 propellant (CT specimen w=54 mm, B=27 mm)

c, mm	f(ξ)	P _{max} , kN	σ _N , MPa	σ _N [∞] , MPa
27	9.66	0.0585	0.0319	0.3078
28	10.24	0.0521	0.0276	0.2826
29	10.88	0.0473	0.0249	0.2703
30	11.59	0.0362	0.0191	0.2209
31	12.38	0.0370	0.0188	0.2330

Table 7. Experimentally evaluated Un-notched strengths for 0,2,3, and 4 years aged samples

Age, years	σ ₀ (MPa)		
	Type-1	Type-2	Type-3
0	0.8502	0.6708	0.7443
2	1.0542	0.7963	1.4308
3	1.1072	0.8326	1.5220
4	1.3317	0.8846	1.7828

Table 8. Estimated characteristic lengths for IFM, PSC & ASC fracture models at c=29 mm

Conditions	Type-1	Type-2	Type-3
IFM	1.8375	2.5138	0.6381
PSC	0.9046	1.2308	0.3173
ASC	3.6749	5.0277	1.2762

5.2 Experimental Evaluation of Parameters for Fracture Models

Fracture toughness evaluated from load-displacement plot as shown in Fig. 4(c) in line with ¹⁷. Evaluated Provisional fracture toughness verified for its compliance to Eqn. (2), Eqn. (3), Eqn. (4). Compliance values are accepted as valid fracture toughness of propellant.

From the valid fracture toughness values, fracture strength was evaluated. Characteristic length for IFM estimated using Eqn.(10). Graphically shown in Fig. 4(d). The experimentally evaluated Characteristic length for fracture models is compiled in Table 8. for the crack length of 29 mm.

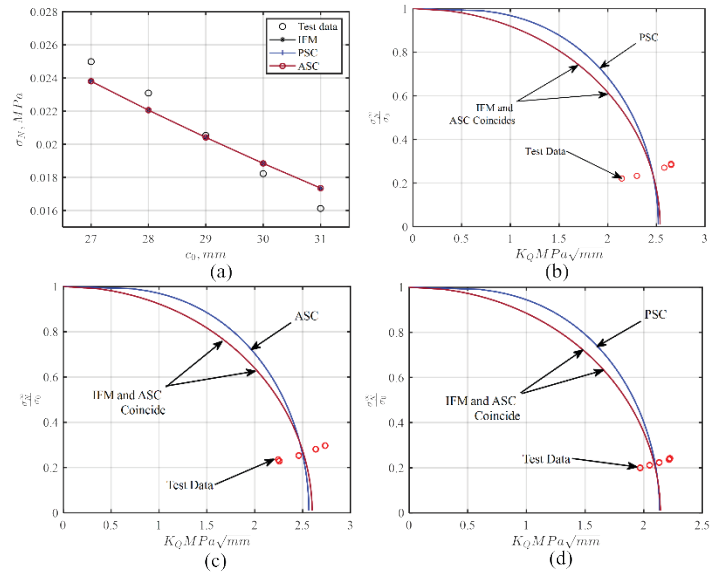


Figure 5. Fracture parameters (a) Notched strength for type-3 propellant; (b) Evaluated FAD for type-1; (c) Evaluated FAD for type-2; and (d) Evaluated FAD for type-3.

Fracture strength of samples from all three types decreases with the increase in notch size as is evident from test results and values predicted from fracture models using evaluated parameters. The observed trends are plotted in Fig. 5(a) for type-3 propellant.

Table 9. Estimated values of fracture parameters K_f(MPa√mm) & m for three models.

Fracture models	Type-1		Type-2		Type-3	
	K _f	m	K _f	m	K _f	m
IFM	2.5375	0	2.5989	0	2.1415	0
PSC	1.7812	0	1.8134	0	1.5101	0
ASC	3.5885	0	3.6754	0	3.0285	0

Parameters of fracture models (IFM, PSC and ASC) evaluated using Eqn. (16) and applying the Newton-Raphson method for all three types of propellant compositions and compiled in Table 9.

With the evaluated parameters, FAD for all cases evaluated and compared in Fig. 5 (b-d). They are in good agreement with the experiment results.

FAD plotted in Fig. 5(b), Fig. 5(c) and Fig. 5(d) for type-1, type-2 and type-3 propellants respectively commonly indicate IFM & ASC are coinciding in predicting the notched strength

Table 10. Experimentally evaluated notched fracture strength for type-1 compared with notched strength evaluated from fracture models with $\sigma_0=1.1072$ (MPa)

Crack length (mm)	σ_N (MPa)			
	Test	IFM	PSC	ASC
27	0.0319	0.0277	0.0277	0.0277
28	0.0276	0.0257	0.0257	0.0257
29	0.0249	0.0238	0.0238	0.0238
30	0.0191	0.0220	0.0220	0.0220
31	0.0188	0.0202	0.0202	0.0202

Table 11. Notched fracture strength for type-2 from test and fracture models with $\sigma_0=0.8326$ (MPa)

Crack length (mm)	σ_N (MPa)			
	Test	IFM	PSC	ASC
27	0.0307	0.0277	0.0277	0.0277
28	0.0275	0.0257	0.0257	0.0257
29	0.0216	0.0238	0.0238	0.0238
30	0.0219	0.0220	0.0220	0.0220
31	0.0185	0.0203	0.0203	0.0203

Table 12. Notched fracture strength for type-3 from test and fracture models with $\sigma_0=1.5220$ (MPa)

Crack length (mm)	σ_N (MPa)			
	Test	IFM	PSC	ASC
27	0.0250	0.0238	0.0238	0.0238
28	0.0231	0.0221	0.0221	0.0221
29	0.0205	0.0204	0.0204	0.0204
30	0.0182	0.0188	0.0188	0.0188
31	0.0161	0.0174	0.0174	0.0174

Table 13. Experimentally evaluated peak load compared with models estimated peak load for type-1, 3-year-old samples.

c (mm)	f(ξ)	$\left(\frac{\sigma_N^\infty}{\sigma_0}\right)$	P_{max} , kN			
			Test	IFM	PSC	ASC
27	9.66	0.278	0.0585	0.0503	0.0504	0.0503
28	10.24	0.255	0.0521	0.0476	0.0476	0.0476
29	10.88	0.244	0.0473	0.0449	0.0449	0.0449
30	11.59	0.199	0.0362	0.0426	0.0425	0.0426
31	12.38	0.210	0.0370	0.0398	0.0397	0.0398

and are also close to experiment results. The observations are in line with Eqn. (19)- Eqn. (21).

The estimates from PSC too are in good agreement with to experiment results. FAD plotted for all three types of samples together for ASC in Fig. 6(a) and results are in line with expectations based on their respective compositions. The plot in Fig. 6(b), for type-1 samples, indicates that the fracture strength of propellant reduces with age. Similar trends were noticed for the other two types of propellants under study, though the margins are different.

6. CONCLUSION

The present study examined experimentally the fracture

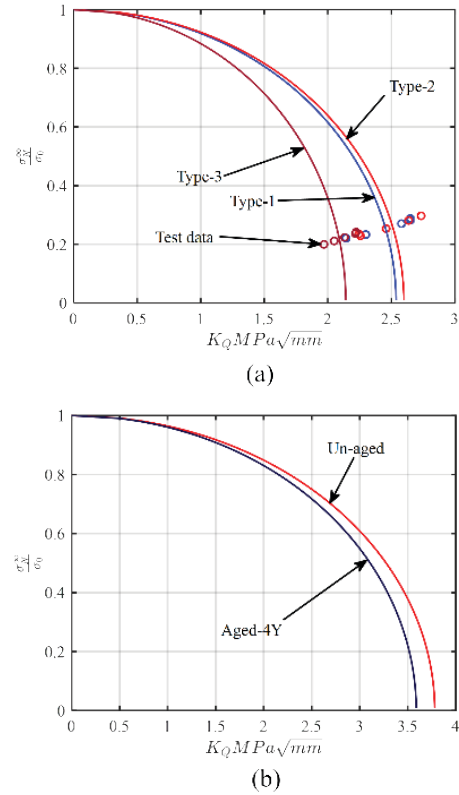


Figure 6. FAD on ASC (a) For type-1, type-2 and type-3 propellant compositions; and (b) FAD for aged samples in ASC for type-1 propellant composition.

behaviour of solid propellant of three different compositions of unaged and naturally aged propellants. The predicted notched strengths of propellant samples by fracture models with experimentally evaluated parameters agree with the experiment results. The results showed that the notched strength decreases with an increase in notch size for all tested compositions. The estimated decrease in notch strength (with an increase in crack size from 27 mm to 31mm) for type-1, type-2 and type-3 propellant are 36.82 %, 39.90 % and 35.47 % respectively estimated from CT specimens. Knowing the notch size, the fracture strength can be estimated with a good level of accuracy. The fracture strengths vary differently with compositions of propellant and test results shows decrease with age. Though, more no of experiments need to be conducted on naturally aged samples to ascertain further the trends noticed. These are planned as future works.

REFERENCES

- Schapery RA. A theory of crack initiation and growth in Viscoelastic Media. International Journal of Fracture. 1975; 1(4): p. 549-562.
- Gledhill RA&KAJ. A unique Fracture Criterion for characterizing the fracture of propellant. Propellant Explosives and Pyrotechnics. 1979; 4(4): p. 73-77.
- Bencher CD,DRH&RRO. Microstructural damage and fracture process in a composite solid propellant. Journal of Spacecraft and Rockets. 1995; 32(2): p. 328-334.
- Liu, C.T. Crack growth behaviour in solid propellant. Engineering Fracture Mechanics. 1997; 56(1): p. 127-

- 135.
5. Rao AS,RV,&RBN. Generation and validation of failure assessment diagram for notched strength prediction of solid propellant tensile specimen. *Material Science and Technology*. 2005; 21(4): p. 488-494.
 6. Newman,J.C. Fracture Analysis of surface and through cracked sheets and plates. *Engineering Fracture Mechanics*. 1973; 5(3): p. 667-689.
 7. Nuismer,R., & Whitney, J. Stress fracture criteria for laminated composites containing stress concentrations. *Journal of Composite Materials*. 1974; 8(3): p. 253-265.
 8. Waddoups ME EJKB. Macroscopic fracture mechanics of advanced composite materials. *Journals of Composite Materials*. 1971; 5(4): p. 446-454.
 9. Khashaba,U.A. Fracture behaviour of Woven Composites containing various cracks geometry. *Journal of Composite Materials*. 2003; 37(1): p. 5-20.
 10. Rao. S,Y,&RBN. Fracture toughness of nitramine and composite solid propellants. *Material Science and Engineering*. 2005; 403(1-2): p. 125-133.
 11. Tussiwand GS,SVE,TR,&DLLT. Fracture Mechanics of Composite Solid Rocket Propellant Grains: Material Testing. *Journal of Propulsion and Power*. 2009; 25(1): p. 60-73.
 12. Whitney JM NR. Stress fracture criteria for laminated composites containing stress concentrations. *journal of composite materials*. 1974; 8(3): p. 253-265.
 13. Rao BN. Fracture of Solid Propellant Grain. *Engineering Fracture Mechanics*. 1992; 43(3): p. 455-459.
 14. Liu.C.T. Effect of Load History on Damage Characteristics near crack tips in a particulate composite material. *International Journal of Damage Mechanics*. 2000; 9(1): p. 40-56.
 15. Max Yen SC,&LCT. Effect of strain rate on the near crack tip behaviour of a particulate composite. *International Journal of Damage Mechanics*. 2000; 9(4): p. 352-377.
 16. Smith C&LCT. Effects of near tip behaviour of particulate composite on classical concepts. *Composite Engineering*. 1991; 1(4): p. 249-257.
 17. Yeh.H.Y LD&LCT. An experimental study of the loading rate effect on the crack growth behaviour in a composite solid propellant. *Journal of Reinforced Plastics and Composites*. 1993; 12(1): p. 48-57.
 18. Patel, Y., Blackman, B. & Williams,J. Determining Fracture Toughness from cutting tests on Polymers. *Engineering Fracture Mechanics*. 2009; 76(18): p. 2711-2730.
 19. Rao, A., Krishna, Y. & Rao,B. Comparison of fracture models to assess the notched strength of composite/solid propellant tensile specimens. *Materials Science and Engineering*. 2004; 385(1-2): p. 429-439.
 20. M. Martínez AJCASJR. On the failure assessment diagram methodology in polyamide 12. 2022; 269.
 21. Ha JS, Kim JH, Yang HY. A study on failure assessment diagrams for a solid propellant. 2012; 16(5).
 22. Jianru Wang PCaXW. Review of the mechanical properties and numerical simulation of composite solid propellants. 2023; 16(21).
 23. Anderson TL. *Fracture Mechanics: Fundamentals and Applications*,4th ed.: CRC Press; 2017.
 24. ASTM E. Standard Test Method for Linear-Elastic Plane-Strain Fracture Toughness K_{Ic} of Metallic Materials. 2009..
 25. NK Srivastava VSbMBPD. The degradation in load carrying capability of delaminated specimens. *Defence Science Journal*. 2025; 75(1): p. 120-128.

CONTRIBUTORS

Shri Deokumar Verma obtained his MTech in SMD from IIT, Kanpur and working as a Scientist 'F' at DRDO. His areas of research include: Development, processing and static testing of large-size solid rocket motors. He also specialises in material characterization.

In the present studies, he formulated and conducted experiments and compiled test results.

Prof S. Bhowmick is an Eminent Professor at the National Institute of Technology, Raipur. His specialized areas include: Formulation and strength evaluation of Functionally Graded Material (FGM), machined design, computational mechanics, FEM and fluid structure interactions.

In the current study he reviewed test plans for each test, experiment results and final compilations.

Dr. MVL Ramesh is a General Manager of SF Complex, DRDO Jagdalpur. His areas of research include: Development, processing and testing of large solid rocket motors.

He has been a guiding force behind the present research work and reviewed the compilation.

Dr Vivek Gaba is presently working as an Associate Professor at the National Institute of Technology, Raipur. His specialized areas include: Heat transfer, thermodynamics, refrigeration and air conditioning, non-conventional sources of energy and numerical methods.

He guided at each step of test result analysis and paper compilation.